ORIGINAL PAPER

Numerical simulations on influence of urban land cover expansion and anthropogenic heat release on urban meteorological environment in Pearl River Delta

Ning Zhang[1,2] · Xuemei Wang[3] · Yan Chen[4] · Wei Dai[3] · Xueyuan Wang[5]

Abstract Urbanization is an extreme way in which human being changes the land use/land cover of the earth surface, and anthropogenic heat release occurs at the same time. In this paper, the anthropogenic heat release parameterization scheme in the Weather Research and Forecasting model is modified to consider the spatial heterogeneity of the release; and the impacts of land use change and anthropogenic heat release on urban boundary layer structure in the Pearl River Delta, China, are studied with a series of numerical experiments. The results show that the anthropogenic heat release contributes nearly 75 % to the urban heat island intensity in our studied period. The impact of anthropogenic heat release on near-surface specific humidity is very weak, but that on relative humidity is apparent due to the near-surface air temperature change. The near-surface wind speed decreases after the local land use is changed to urban type due to the increased land surface roughness, but the anthropogenic heat release leads to increases of the low-level wind speed and decreases above in the urban boundary layer because the anthropogenic heat release reduces the boundary layer stability and enhances the vertical mixing.

✉ Xuemei Wang
eeswxm@mail.sysu.edu.cn

[1] Institute of Climate & Global Change Research and School of Atmospheric Sciences, Nanjing University, Nanjing 210023, China

[2] Jiangsu Collaborative Innovation Center for Climate Change, Nanjing 210023, China

[3] School of Environmental Science and Engineering, Sun Yat-sen University, Guangzhou 519001, China

[4] Jiangsu Climate Center, Nanjing 210002, China

[5] School of Atmospheric Sciences, Nanjing University, Nanjing 210023, China

1 Introduction

Urbanization is a very quick process in which human being changes the characteristics of land surface, including the dynamical features, radioactive features, and thermal features. These modifications change the interactions between land surface and the atmosphere, urban areas are always characterized by higher turbulent sensible heat flux because of the high heat captivity and low latent heat flux because the urban surface is modified to impervious surface and the local evaporation is reduced. Such a change of local land use/land cover also changes the local micro-climate environment, and urban heat island (UHI) is one of the most important phenomena in urban climate. Accompanying with the change of land-atmosphere interactions, urbanization also modifies the urban atmospheric boundary layer, interacts with other mesoscale circulations, changes the precipitation processes, or even impacts regional climate (Kaufmann et al. 2007; Lo et al. 2007; Han and Baik 2008; Trusilova et al. 2008; Wang 2009; Chen et al., 2011a, b; Miao et al. 2011; Feng et al. 2012; Lazzarini et al. 2013; Wang et al. 2013; Yang et al. 2013; Giovannini et al. 2014).

Besides the surface fluxes partition changed by urban land surface radiation/thermal features, the human being activities in urban area also release a lot of waste heat (anthropogenic heat). The anthropogenic heat flux supplies additional energy source in urban area compared to rural/vegetation area and changes the local surface energy balance (Offerle et al. 2005; Smith et al. 2009; Iamarino et al. 2012). Taha (1997) regarded anthropogenic heat flux as one of the important factors which modify urban climate. Many researchers have reported that anthropogenic heat flux can change the local atmospheric circulation and impact regional or even global climate. Narumi et al. (2009) investigated the influence of anthropogenic heat flux on local urban climate in a Japanese megacity, the results indicated that the amount of heat released

is lower at night than during the day, but the temperature rise is nearly three times greater, and the anthropogenic heat flux delayed the onset of land breezes, particularly in a coastal area. Chen et al. (2009) documented that the daily average contribution ratio of anthropogenic heat flux in the winter can reach 54.5 %, compared to 43.6 % in the summer, and the anthropogenic heat flux also strengthens the vertical movement of urban surface air flow, changing the urban heat island circulation. Block et al. (2004) and Feng et al. (2012) found that anthropogenic heat flux has influence on regional climate. Flanner (2009) integrated anthropogenic heat flux in global climate models and found that anthropogenic heat flux caused significant increases in annual mean temperature and planetary boundary layer (PBL) height occur over grid cells where present-day anthropogenic heat flux exceeds 3.0 W m^{-2}; these influences may have further impacts on chemistry-climate processes.

Anthropogenic heat flux is important for both urban atmospheric boundary layer processes and regional climate, while it is difficult to measure it directly. Usually, it is estimated with a top-down method using energy consumption statistics,

population data, and so on (Sailor and Lu 2004; Pigeon et al. 2007; Lee et al. 2009; Smith et al. 2009; Allen et al. 2011; Sailor 2011; Chen et al. 2012; Iamarino et al. 2012; Quah and Roth 2012). The anthropogenic heat flux varies spatially and temporally. Iamarino et al. (2012) documented that the annual mean anthropogenic heat flux for Greater London is 10.9 W m^{-2} for 2005–2008, with the highest peaks in the central activities zone (CAZ). Ferreira et al. (2011) estimated the anthropogenic heat flux in Sao Paulo is about 20 W m^{-2}, and its diurnal variation has three peaks due to the traffic waste heat release. Lee et al. (2009) calculated the anthropogenic heat flux in Gyeong-In area of Korea, the results showed that annual mean anthropogenic heat emissions in Seoul, Incheon, and Gyeonggi are found to be 55, 53, and 28 W m^{-2}, The maximum annual mean anthropogenic heat emission averaged over a grid area of 1 × 1 km in each district is found to be 27 W m^{-2} in Seoul, 320 W m^{-2} in Incheon, and 198 W m^{-2} in Gyeonggi. Allen et al. (2011) developed the large-scale urban consumption of energy (LUCY) model which simulates all components of anthropogenic heat flux from the global to individual city scale and found that the

Fig. 1 Simulation domains: **a** topography of the 18-km-resolution domain, **b** topography, **c** land cover, **d** anthropogenic heat release of the 3-km-resolution domain
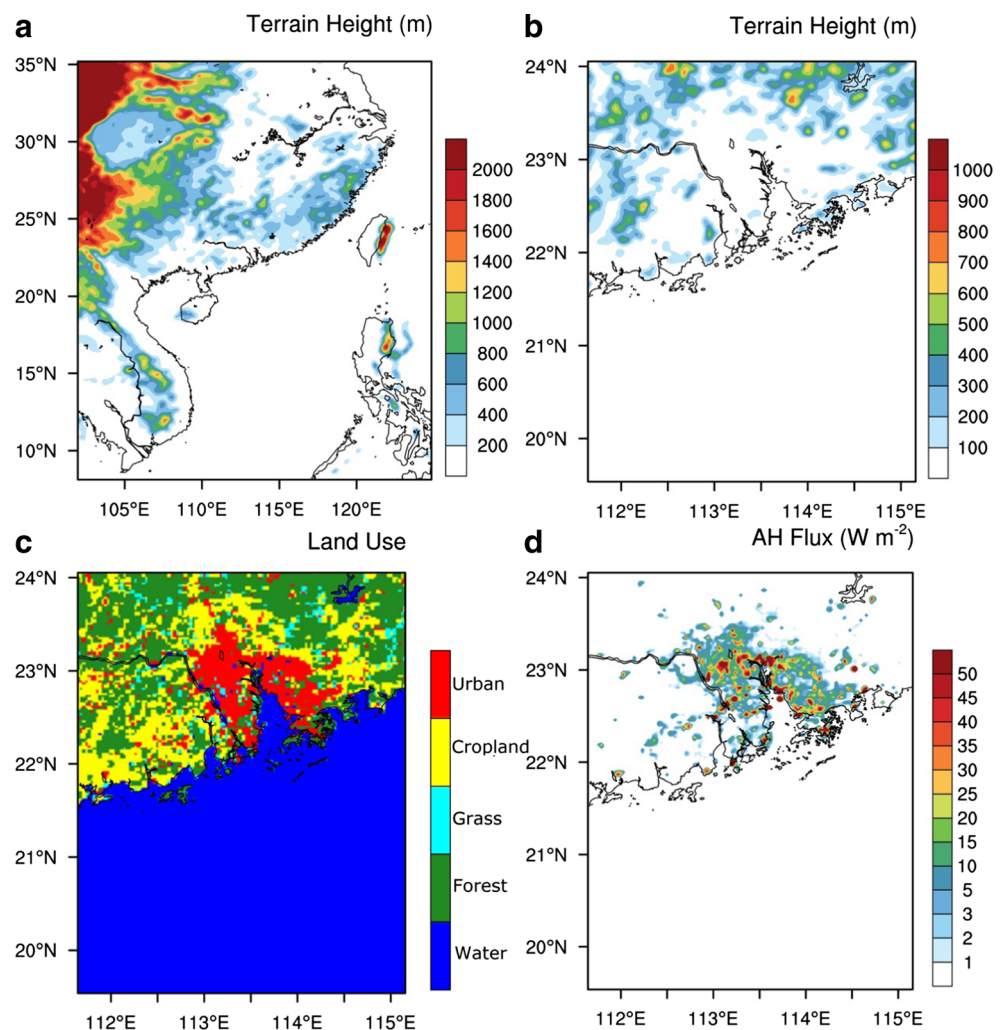
Table 1 Comparison of the simulated and observed near surface meteorological parameters

	Experiment	Mean$_{SIM}$	Mean$_{OBS}$	Bias	R	RMSE	IOA
Air temperature at 2 m (°C)	AH	18.45	19.02	−0.57	0.85	1.24	0.89
	uniAH	18.45	19.02	−0.57	0.85	1.26	0.88
	URB	18.03	19.02	−0.99	0.84	1.44	0.88
	noURB	17.22	19.02	−1.80	0.83	1.98	0.86
Wind speed at 10 m (m s^{-1})	AH	3.86	2.89	0.87	0.74	1.70	0.71
	uniAH	3.68	2.89	0.79	0.72	1.65	0.71
	URB	3.68	2.89	0.79	0.72	1.80	0.71
	noURB	4.09	2.89	1.20	0.69	1.91	0.69
Relative humidity at 2 m (%)	AH	54.27	49.03	5.24	0.87	9.79	0.88
	uniAH	53.95	49.03	4.91	0.87	9.51	0.88
	URB	56.75	49.03	7.72	0.85	11.89	0.87
	noURB	60.04	49.03	11.01	0.84	13.15	0.85
Specific humidity at 2 m (g kg^{-1})	AH	8.13	8.21	−0.09	0.82	1.09	0.91
	uniAH	8.04	8.21	−0.17	0.78	1.22	0.88
	URB	8.16	8.21	−0.05	0.80	1.15	0.90
	noURB	8.79	8.21	0.58	0.79	1.32	0.87

Mean$_{SIM}$ simulated mean value, *Mean$_{OBS}$* observed mean value, *Bias* simulated value minus observed value, *R* correlation coefficient, *RMSE* root mean square error, *IOA* index of agreement

global mean urban anthropogenic heat flux has a diurnal range of 0.7–3.6 W m^{-2} and the highest individual grid cell heat fluxes in urban areas were located in megacities. Wang and Wang (2011) estimated the anthropogenic heat flux in Guangzhou City and found the averaged flux intensity was about 41.1 W m^{-2} in 2010.

Anthropogenic heat flux has been an important energy source for the urban surface energy balance (Ichinose et al. 1999; Lee et al. 2009; Sailor 2011; Iamarino et al. 2012), and it must be considered in the numerical models for urban boundary layer structures and urban climate simulations or even in regional climate simulations (Ichinose et al. 1999; Chen et al.

Fig. 2 Eight-day averaged simulated horizontal distribution of **a** temperature at 2 m, **b** wind speed at 10 m, **c** relative humidity at 2 m, **d** specific humidity at 2 m over the urbanized area. (The 8-day averaged observations are *marked* and the water area is set as *blank*)
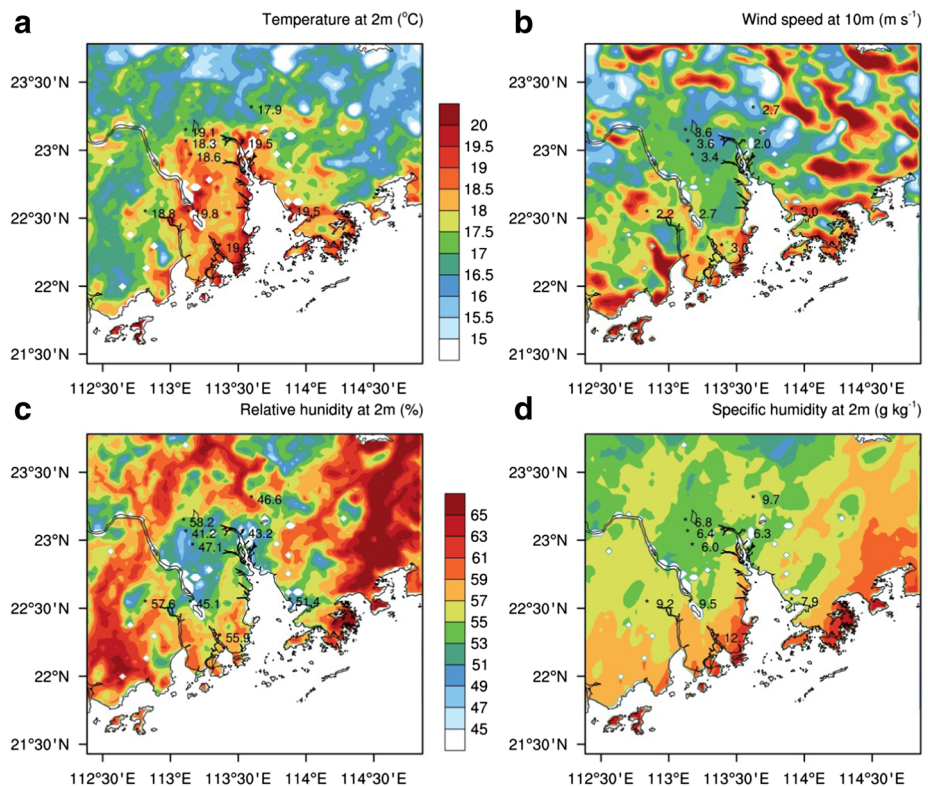
2009; Flanner 2009; Narumi et al. 2009; Krpo et al. 2010). Because of the difficult to get detailed anthropogenic heat flux data, in many previous numerical modelling on urban climate, the influence of anthropogenic heat flux is not considered (Zhang et al. 2010, 2012; Wang et al. 2013), or it is considered in a crude way depending on the urban building cover density (Chen et al. 2009; Miao et al. 2009; Feng et al. 2012) as in current Weather and Forecasting (WRF) model releases. In the real world, the anthropogenic heat flux intensity may be different over different urban function zones, even with the same building density. In this paper, detailed independent anthropogenic heat flux spatial distributions including industrial emission, traffic emission, and civil emission and their temporal variations are considered in the WRF model. With the WRF model, the impact of both urban area expansion and anthropogenic heat flux are considered to study the urban meteorological conditions and boundary layer structure in the Pearl River Delta, China, and their contributions to the modification of atmospheric boundary layer characteristics are compared.

2 Numerical experiments design

In this paper, the WRF model (version 3.4.1) with the ARW core is selected as the numerical tool. WRF is based on a fully compressible and no hydrostatic dynamic core and suitable for atmospheric numerical modelling from large eddy simulation to global scale (http://www.wrf-model.org). The simulation domain covers the whole Pearl River Delta, China, one of the most urbanized areas in China, which contains a population of 56 million and nearly 70 % is urban residence; this area also contributes nearly 15 % of Chinese GDP. Two-domain nesting simulations are carried out, the horizontal resolution of outer/inner domain is 18/3 km. The inner domain is centered at (113.4 E, 21.8 N) as shown in Fig. 1. The vertical grid system consists of 38 full-sigma levels, and under this vertical resolution, there are about 15 layers below 2000 m. The model top is located at 50 hPa. The lowest full-sigma level above the ground is 0.995, and the lowest half-sigma level height is approximately 35 m above ground.

Fig. 3 Eight-day averaged differences in air temperature at 2 m: **a** the URB experiment minus the NOURB experiment, **b** the AH experiment minus the URB experiment, **c** the AH experiment minus the URB experiment, **d** the UNIAH experiment minus the URB experiment
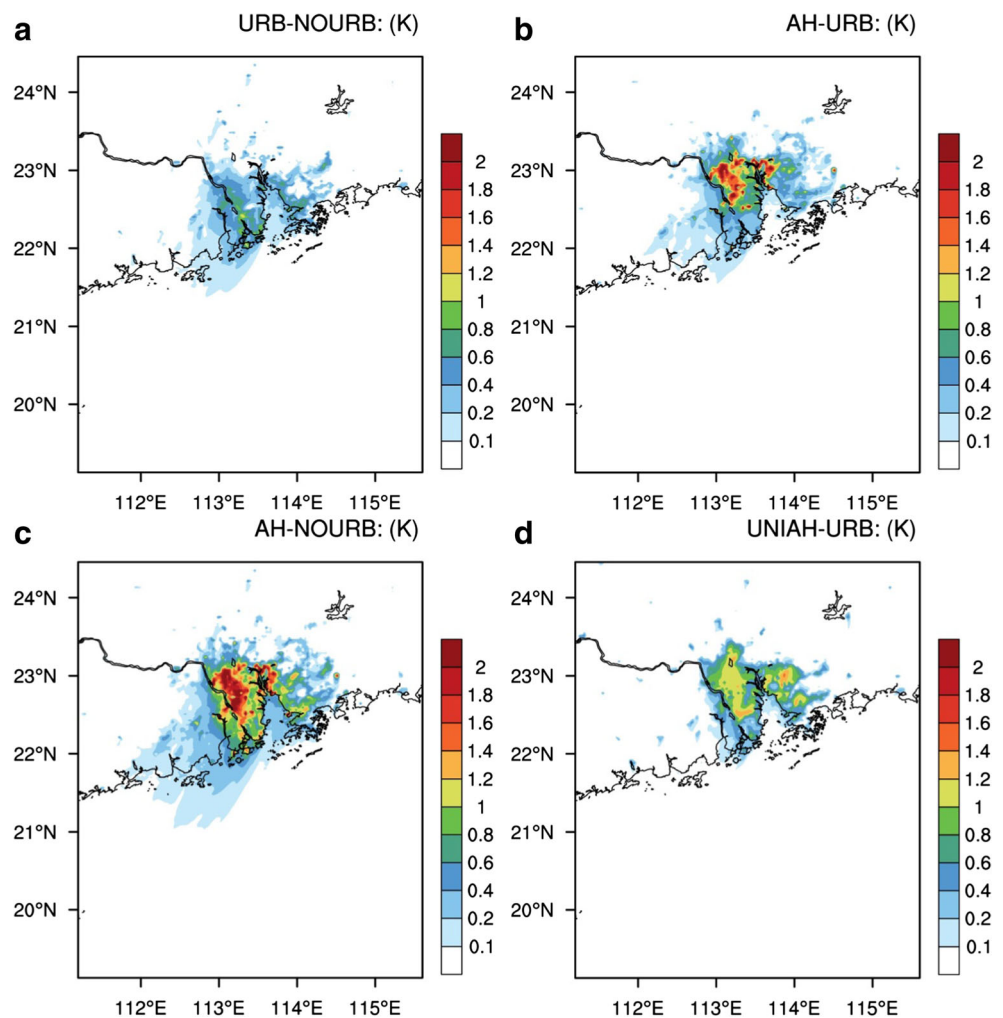
The model integrations are conducted for 9 days from 0000UTC 26 October to 0000 UTC 04 November 2010. The first day is set as a "spin-up" period, and results of the last 8 days (from 0000UTC 27 October to 0000UTC 04 November) are used for the analysis in this paper. In these days, the Pearl River Delta was controlled by a stable high pressure and the background wind is form north-northeast. Under such a synoptic background, the air pollutant is transported from north China and may cause hazard air pollution episode in this area. The initial and boundary conditions are provided by the 1° * 1° NCEP FNL data and the boundary conditions are forced every 6 h.

The physics package used in the simulations includes the RRTMG (Rapid Radiative Transfer Model for GCMs) (Mlawer et al. 1997) longwave radiation and Goddard shortwave radiation processes (Chou et al. 1999), Bett-Miller-Janjic cumulus scheme (only for the outer domain), Lin microphysics scheme (only for the inner domain), and the URB land-surface model (LSM), which coupled a single-layer urban canopy model (UCM) (Chen et al. 2011a, b) to represent for the urban buildings' impacts on radiation transporting, urban heat storage, building surface energy budgets, and urban flows.

Three numerical experiments are designed to study the impacts of urban land cover expansion and anthropogenic heat flux release on urban boundary layer. In the numerical experiment AH, the satellite-observed 15-s resolution MODIS land use type product in 2010 are used to represent the current urbanization conditions. The anthropogenic heat release in the whole simulation domain is described as a four-dimensional array including the location (longitude, latitude, and height) and time information. The anthropogenic heat flux intensity is shown as in Fig. 1d, which is estimated with local energy consumption, population, and GDP distribution from the statistical data of 2010 as described in Chen et al. (2009) and Wang and Wang (2011). The total industrial waste heat release is calculated with total industrial coal consumption and industrial energy utility efficiency; for the living activities heat release, annual living consumption of coal gas, natural gas, and total electricity consumption are converted to standard coal consumption, and then living activities waste-heat release is estimated with the coal consumption amount and energy

Fig. 4 a–d Same as Fig. 2 but for the relative humidity at 2 m
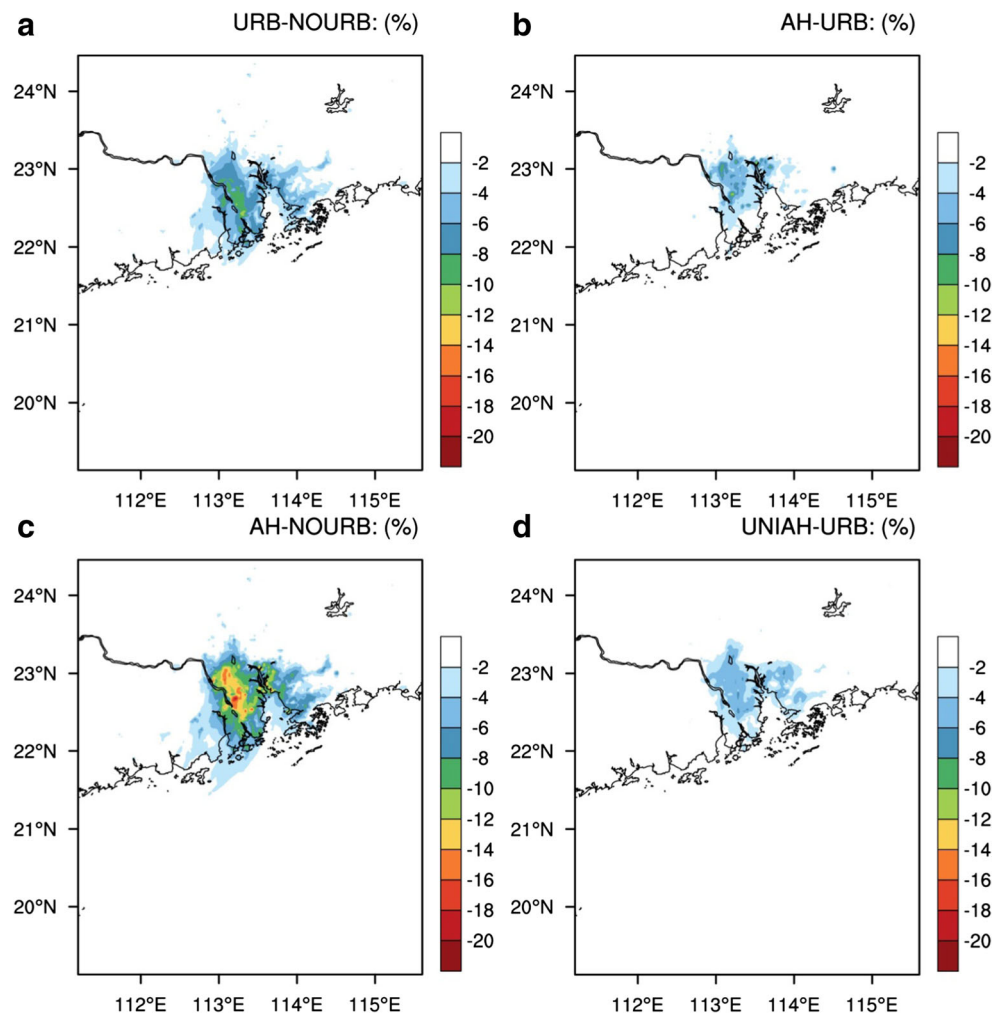
utility efficiency; for traffic heat release estimate, the total gasoline consumption is calculated with the total vehicle number, annual average running distance, and average gasoline consumption rate. The maximum intensity of the total heat release (including industrial heat, living activities, and traffic heat) is 405 W m^{-2} from an industrial park. Due to the lack of related information, all traffic and living emission are assumed to be released on ground surface and added as energy sources in the surface energy balance processes; the industrial emission is set to the first level of the atmosphere model in the prediction equation of air temperature. The time-variations of anthropogenic heat release are not considered in current simulations due to the lack of detailed information. In the numerical experiment URB, only the current urban land cover is considered and the anthropogenic heat flux is set to zero. The experiment NOURB is based on the URB experiment, and the urban land use is replaced by cropland, the nearest rural area land use, to remove the influence of urban land cover. To compare the modified anthropogenic heat release scheme with the default one in WRF, the UNIAH experiment is designed; in this experiment, the total amount of

anthropogenic heat flux is averaged to each urban grid cell, and the current urban land cover from MODIS observation is also considered.

3 Results

3.1 Evaluation of near-surface meteorological field simulations

The hourly air temperature at 2 m, wind speed at 10 m, relative humidity at 2 m observed at the 9 meteorological stations (7 stations locating in the urbanized area and 2 in the suburban/ rural area) in the last 8 simulated days are compared to the WRF outputs to evaluate the model performance as listed in Table 1. The 8-day averaged horizontal distributions of temperature at 2 m, wind speed at 10 m, relative humidity at 2 m, and specific humidity at 2 m from the experiment AH are shown in Fig. 2, and the respective observations are also marked. The experiment AH produces the best simulation results among the four numerical experiments and can capture

Fig. 5 a–d Same as Fig. 2 but for the wind speed at 10 m
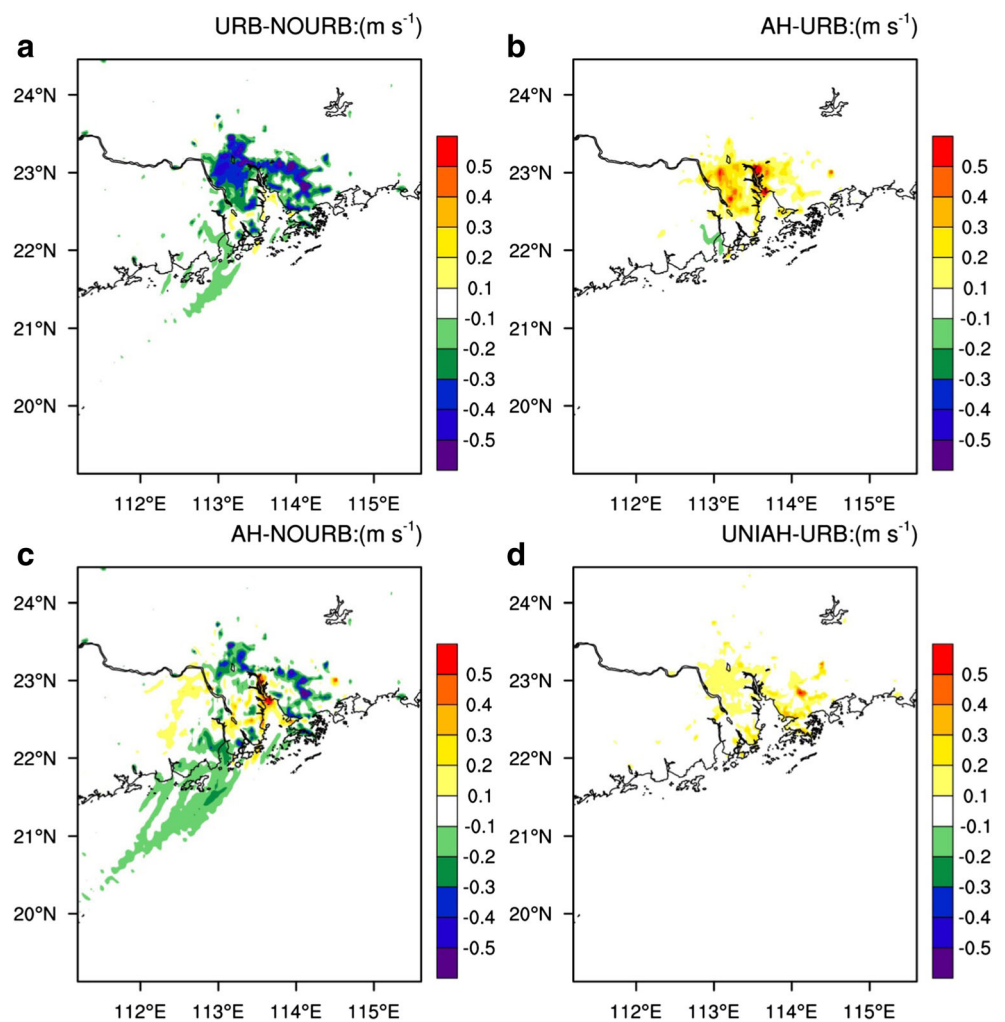
the surface meteorological characteristics well, even though the meteorological observations near high anthropogenic heat release area is sparse. Both simulations in the experiment AH and observations show that the atmosphere over urban area is warmer and drier than suburban/rural area. All experiments underestimate the near-surface air temperature. The experiment NOURB outputs the largest bias of −1.80° because it does not consider the impact of urban canopy and anthropogenic release. The simulations of near-surface temperature are improved when considering the urbanization influence with the single-layer urban canopy model; this is consistent with previous studies (Miao et al. 2009; Salamanca et al. 2011). The experiments AH and UNIAH produce better simulations of near-surface air temperature when the anthropogenic heat release is considered. In the experiments AH and UNIAH, the biases and correlation coefficients are the same, and the experiment AH has a smaller RMSE and higher IOA than the UNIAH experiment.

All experiments overestimate the wind speed at 10 m, because the observation of wind speed is impacted directly by local surrounding environment. When considering the impact of urbanization, WRF model outputs a smaller bias, and the biases in the experiments AH, UNIAH, URB, and NOURB are 0.97, 079, 0.79, and 1.20 m s^{-1}, respectively. The impact of anthropogenic heat release spatial distribution on wind fields is small; the simulated bias of experiment AH simulate is slightly greater than that in experiment UNIAH, but the RMSE decreases and correlation coefficient and IOA increase.

All experiments also overestimate the relative humidity at 2 m, and the results also demonstrate that the considering of anthropogenic heat release and urban land cover will improve the simulations on relative humidity. The bias of the experiment AH is 5.24 % compared to the bias of 11.01 % in experiment NOURB and 7.72 % in the experiment URB.

3.2 Influences on near-surface meteorological fields

In this paper, the changes of meteorological fields among different experiments are used to measure the influence of urbanization-induced land use/land cover change and different parameterization schemes of anthropogenic heat flux in WRF. Figure 3 illustrates the 8-day averaged differences in air temperature at 2 m (T2m) among different experiments. Both the urbanization-induced land use change and anthropogenic heat release lead to temperature increasing, and the temperature increasing is much stronger over the urban area than the other parts in the simulation domain. The mean increase of T2m between the URB experiment and NOURB experiment is 0.03 K over the whole simulation domain and 0.23 K over the urban area. Such a warming effect of urbanization in this area has also been documented by Lo et al. (2007), Wang et al. (2013), and Li et al. (2014). The warming effect in this paper

is weaker than these results in Lo et al. (2007), Wang et al. (2013), and Li et al. (2014), because the urbanization influence not only impacted by the urban canopy processes but also other processes including the synoptic/climate background, the soil moist conditions, and so on. Simulations with anthropogenic result in higher temperature, the mean increase of T2m between the AH experiment and URB experiment is 0.05 K over the whole simulation domain and 0.69 K over the
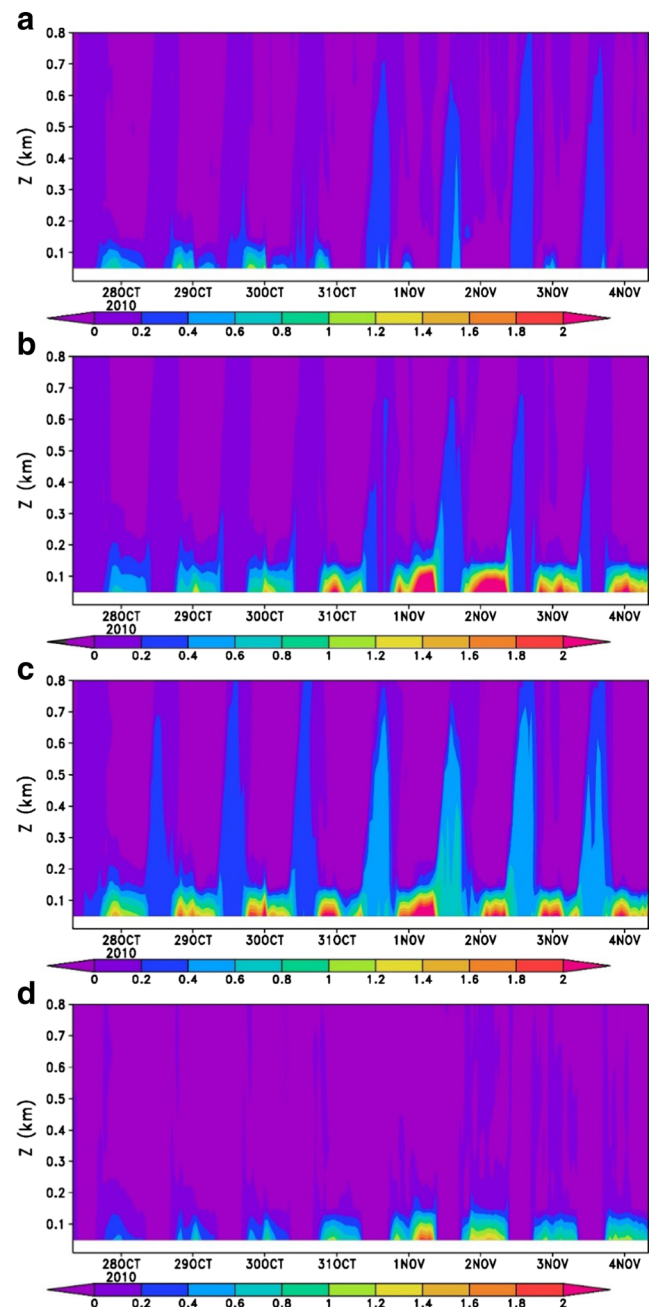

Fig. 6 Differences in spatial averaged vertical potential temperature profiles over urban area: **a** the URB experiment minus the NOURB experiment, **b** the AH experiment minus the URB experiment, **c** the AH experiment minus the NOURB experiment, **d** the UNIAH experiment minus the URB experiment

urban area. The mean increase of T2m between the AH experiment and NOURB experiment is 0.08 K over the whole simulation domain and 0.93 K over the urban area, implying that anthropogenic heat release is a stronger factor of urban heat island in this episode, which contributes 74 % of the UHI intensity in these simulations; this is also found in other cities in China (Chen et al. 2009). The simulation assuming a spatially-homogeneous anthropogenic heat release produce a slightly weaker temperature increasing over the whole domain but stronger UHI, and the mean increase of T2m between the UNIAH experiment and URB experiment is 0.04 K over the whole simulation domain and 0.75 K over the urban area, compared to 0.05 and 0.69 K between the AH experiment and URB experiment. Anthropogenic heat release also contributes greatly on the maximum temperature increasing in our simulations, the maximum temperature bias is 1.15 K (3.37, 3.67, 1.52 K) between the URB (AH, AH, UNIAH) experiment and NOURB (URB, NOURB, URB), respectively. The AH experiments outputs the highest temperature increase, because anthropogenic heat release is concentrated in the industrial regions in this experiment as shown in Fig. 1d.

The land use is modified from vegetation cover to impervious material; this will reduce the evaporation and transpiration in urban area and reduce the near-surface air humidity. The simulation results show that urbanization contributes to most of the changes in near-surface specific humidity; the mean differences in specific humidity at 2 m over urban area are -0.50 g kg^{-1} (0.03, -0.47, -0.02 g kg^{-1}) between the URB (AH, AH, UNIAH) experiment and NOURB (URB, NOURB, URB), respectively. The influence of anthropogenic heat releases on near-surface specific humidity is very weak, but near-surface relative humidity changes due to the changes in near-surface air temperature (Fig. 4). The mean differences in relative humidity at 2 m over urban area are -4.7 % (-2.5, -7.2, -3.4 %) between the URB (AH, AH, UNIAH) experiment and NOURB (URB, NOURB, URB); the mean differences in relative humidity at 2 m over the whole domain 3 are -0.4, -0.25, -0.7 and -0.2 %, respectively.

The urbanization processes, accompanied with buildings, increase the surface roughness and reduce the near-surface wind speed (Trusilova et al. 2008; Sugawara and Narita 2009; Zhang et al. 2010; Hou et al. 2013; Wang et al. 2013;

Fig. 7 a–d Same as Fig. 2 but for the planetary boundary layer height
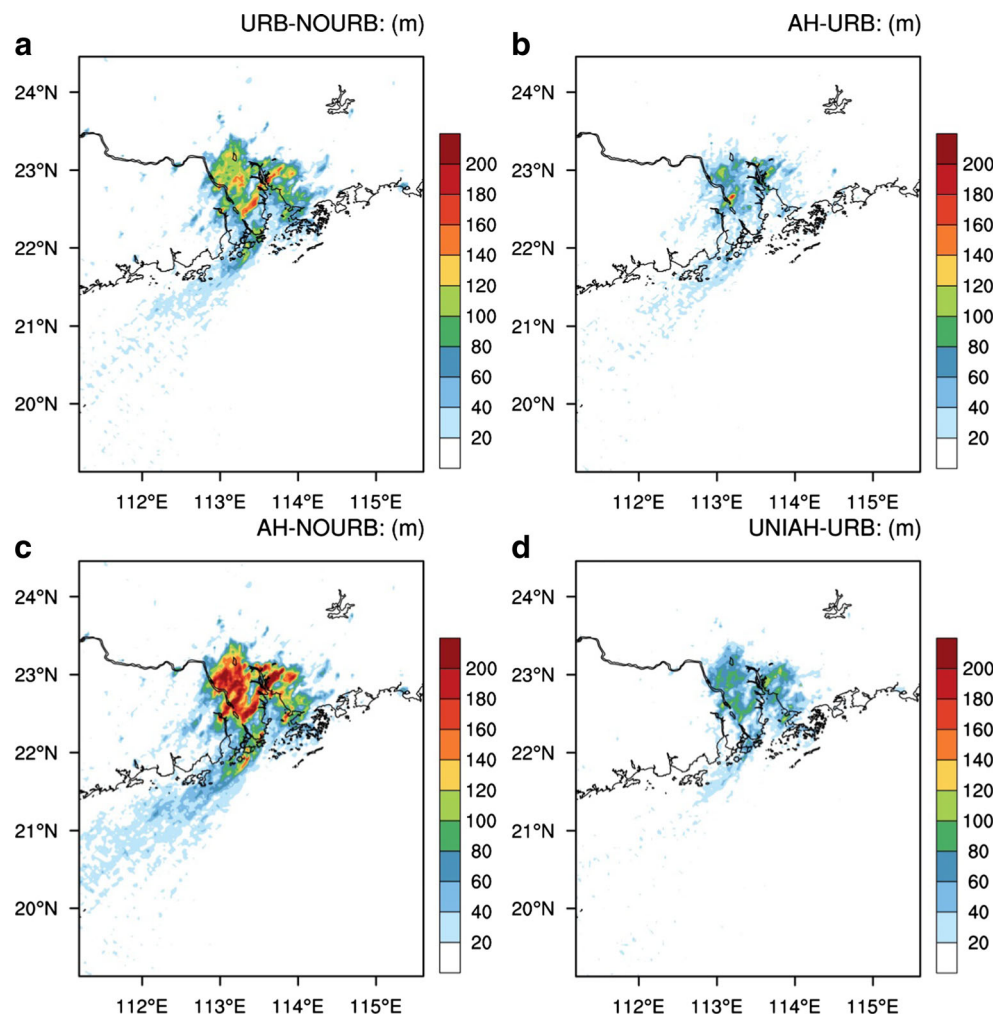
Kanda et al. 2013; Peng and Sun 2014), which is also demonstrated in our simulations (Fig. 5). The differences in wind speed at 10 m between the URB experiment and NOURB experiment is −0.27 m s^{-1} over urban area and the maximum wind speed decreasing is 1.13 m s^{-1}. The impact of anthropogenic heat release shows opposite contribution on near-surface wind speed; near-surface wind speed increases in the AH experiment and UNIAH experiment compared to that in the URB experiment, and the difference in near-surface wind speed between the AH/UNIAH experiment and the URB experiment is 0.23/0.12 m s^{-1}. The combined influence of both land use change and anthropogenic heat release show a weaker wind speed reduction, and the mean difference in near-surface wind speed between the AH experiment and the NOURB experiment is −0.12 m s^{-1} over the urban area.

3.3 Influences on boundary layer structures

Both land use change and anthropogenic heat release increase the near-surface temperature as discussed in section 3.2 and this will reduce the stability of the atmospheric boundary layer. Figure 6 illustrates the vertical changes of potential temperature over the urban area. The large part of increased potential temperature by land use change and anthropogenic heat release occurs at the bottom part of the planetary boundary layer below 300 m. The impact height becomes higher on November 1 and 2 when the synoptic background wind is relative weak.

Increased potential temperature at the bottom layer of planetary boundary layer leads to an increasing of the planetary boundary layer height (PBLH) (Fig. 7). The WRF model diagnoses PBLH based on the simulated turbulent kinetic energy profiles in Mellor-Yamada-Jianic PBL parameterization scheme (LeMone et al., 2013). The simulated PBLH increases in each sensitivity experiments as compared to the NOURB experiment, and the spatial distributions of these changes are very inhomogeneous; the urban area contributes to most of the PBLH increasing. The mean difference between the URB experiment and NOURB experiment is 6.6 m over the whole simulation domain and 79.8 m over the urban area. The uniform anthropogenic heat release experiment (the UNIAH experiment) shows a higher PBLH increasing than the real spatial distribution experiment (the AH experiment); the mean difference between the UNIAH experiment and URB experiment is 3.8 m over the whole simulation domain and 49.8 m over the urban area, and the mean difference between the AH experiment and URB experiment is 2.6 m over the whole simulation domain and 39.7 m over the urban area. The combined contributions of anthropogenic heat release and land use change leads to a stronger increasing of PBLH, and the mean difference between the AH experiment and NOURB experiment is 10.4 m over the whole simulation domain and 112.6 m over the urban area. Even in the urban area, the PBLH

increasing is inhomogeneous, and the maximum of PBLH difference between the URB (AH, AH, UNIAH) experiment and NOURB (URB, NOURB, URB) are 190.8, 187.9, 306.0, and 165.5 m, respectively.

The modifications in the vertical distribution of potential temperature also affect the wind field simulations. The increasing of potential temperature at the bottom level of PBL destabilizes the boundary layer and enhances the vertical mixing, and at the same time, the wind speed usually increases with height in the surface layer; this increases the surface wind speed and decreases the wind speed at above level. The simulations in different experiments also prove this (Fig. 8). This
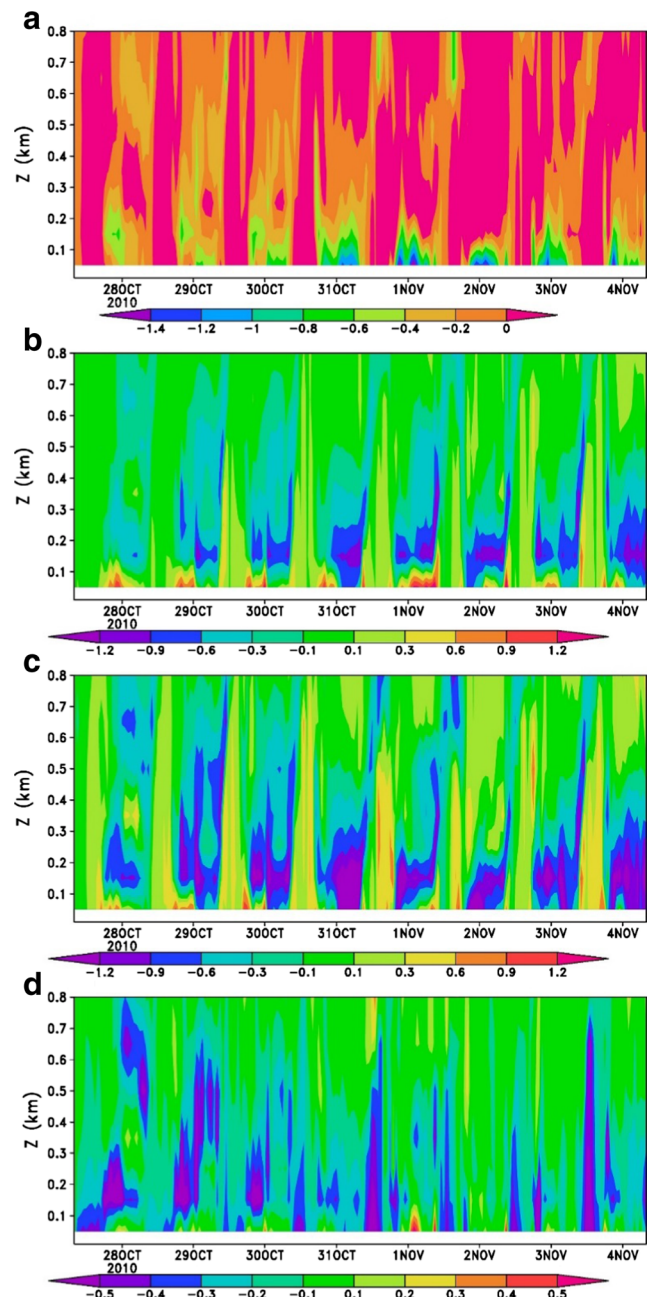

Fig. 8 a–d Same as Fig. 6 but for the vertical wind speed profiles

phenomenon is not been observed in the differences of vertical wind speed distribution between the URB experiment and the NOURB experiment, because the surface wind speed is reduced strongly by the increasing surface roughness over urban area. But the differences in vertical profiles of wind speed between the AH experiment and the URB experiment and the differences between the UNIAH experiment and the URB experiment both show clear decreases in wind speed at the height of about 200 m and increases in surface wind speed at the same time.

4 Conclusions and discussions

The WRF model is modified to consider the real spatial distribution of anthropogenic heat release, and a series of numerical simulations are carried out for the Pearl River Delta area, which is one of the most important city clusters in China. The simulations' results show the following:

1. Anthropogenic heat release is an important factor contributing to the urban heat island intensity in Pearl River Delta, China. The WRF model produces better simulations for near-surface meteorological fields when a more realistic anthropogenic heat release is considered in the model.
2. Both urbanization and anthropogenic heat release lead to surface temperature increases and cause urban heat island; the anthropogenic heat release contribute to nearly 75 % of the urban heat island intensity in our simulations. Anthropogenic heat release has little impacts on near-surface specific humidity, but still affects near-surface relative humidity by changing local near-surface temperature. The urbanization-induced land use change causes decreases in near-surface wind speed, while anthropogenic heat release causes increases in near-surface wind speed.
3. Both urbanization and anthropogenic heat release warm the near-surface atmosphere and reduce the stability of the atmospheric boundary layer and increase the PBL height in our simulations. These processes also impact the wind fields in urban boundary layer. In our simulations, the near-surface wind speed decreases after the local land use is changed to urban type due to the increased land surface roughness, but the anthropogenic heat release leads to increases of the low-level wind speed and decreases above in the urban boundary layer because the anthropogenic heat release reduces the boundary layer stability and enhances the vertical mixing.

Anthropogenic heat release is a very important energy source of urban surface energy balance; it will impact urban meteorological environment and boundary layer structure directly. Anthropogenic heat release in urban area is very complicated because it varies substantially in space and time The parameterization scheme of anthropogenic heat release in numerical models is very difficult because the processes is so complicated and difficult to be measured. In this paper, only the spatial distribution impact of anthropogenic heat release is discussed. The diurnal variations are not considered, and this may amplify the impacts at night and underestimate the impacts in the daytime because previous studies show that the AH release is stronger in the daytime than at nighttime (Chen et al. 2009, Miao et al. 2009). The impacts of temporal variations (such as diurnal, weekly, monthly even annual circle) should be considered in the future studies.

References

Allen L, Lindberg F, Grimmond CSB (2011) Global to city scale urban anthropogenic heat flux: model and variability. Int J Climatol 31: 1990–2005. doi:10.1002/Joc.2210

Block A, Keuler K, Schaller E (2004) Impacts of anthropogenic heat on regional climate patterns. Geophys Res Lett 31 doi:Artn L12211

Chen Y, Jiang WM, Zhang N, He XF, Zhou RW (2009) Numerical simulation of the anthropogenic heat effect on urban boundary layer structure. Theor Appl Climatol 97:123–134. doi:10.1007/s00704-008-0054-0

Chen F et al. (2011a) The integrated WRF/urban modelling system: development, evaluation, and applications to urban environmental problems. Int J Climatol 31:273–288. doi:10.1002/Joc.2158

Chen F, Miao S, Tewari M, Bao J-W, Kusaka H (2011b) A numerical study of interactions between surface forcing and sea breeze circulations and their effects on stagnation in the greater Houston area. J Geophys Res 116(D12)

Chen B, Shi GY, Wang B, Zhao JQ, Tan SC (2012) Estimation of the anthropogenic heat release distribution in China from 1992 to 2009. Acta Meteorol Sin 26:507–515. doi:10.1007/s13351-012-0409-y

Chou M-D, Kyu-Tae L, Si-Chee T, Qiang F (1999) Parameterization for cloud longwave scattering for use in atmospheric models. J Clim 12: 159

Feng JM, Wang YL, Ma ZG, Liu YH (2012) Simulating the regional impacts of urbanization and anthropogenic heat release on climate across China. J Clim 25:7187–7203. doi:10.1175/Jcli-D-11-00333.1

Ferreira MJ, de Oliveira AP, Soares J (2011) Anthropogenic heat in the city of Sao Paulo, Brazil. Theor Appl Climatol 104:43–56. doi:10.1007/s00704-010-0322-7

Flanner MG (2009) Integrating anthropogenic heat flux with global climate models. Geophys Res Lett 36 doi:Artn L02801

Giovannini L, Zardi D, de Franceschi M, Chen F (2014) Numerical simulations of boundary-layer processes and urban-induced alterations in an Alpine valley. Int J Climatol 34(4):1111–1131

Han J-Y, Baik J-J (2008) A theoretical and numerical study of urban heat island-induced circulation and convection. J Atmos Sci 65:1859–1877. doi:10.1175/2007jas2326.1

Hou A, Ni G, Yang H, Lei Z (2013) Numerical analysis on the contribution of urbanization to wind stilling: an example over the Greater Beijing Metropolitan Area. J Appl Meteorol Climatol 52:1105–1115. doi:10.1175/jamc-d-12-013.1

Iamarino M, Beevers S, Grimmond CSB (2012) High-resolution (space, time) anthropogenic heat emissions: London 1970–2025. Int J Climatol 32:1754–1767. doi:10.1002/Joc.2390

Ichinose T, Shimodozono K, Hanaki K (1999) Impact of anthropogenic heat on urban climate in Tokyo. Atmos Environ 33:3897–3909. doi:10.1016/S1352-2310(99)00132-6

Kanda M, Inagaki A, Miyamoto T, Gryschka M, Raasch S (2013) A new aerodynamic parametrization for real urban surfaces boundary-layer. Meteorology 148:357–377. doi:10.1007/s10546-013-9818-x

Kaufmann RK, Seto KC, Schneider A, Liu ZT, Zhou LM, Wang WL (2007) Climate response to rapid urban growth: evidence of a human-induced precipitation deficit. J Clim 20:2299–2306. doi:10.1175/Jcli4109.1

Krpo A, Salamanca F, Martilli A, Clappier A (2010) On the impact of anthropogenic heat fluxes on the urban boundary layer: a two-dimensional numerical study boundary-layer. Meteorology 136:105–127. doi:10.1007/s10546-010-9491-2

Lazzarini M, Marpu PR, Ghedira H (2013) Temperature-land cover interactions: the inversion of urban heat island phenomenon in desert city areas. Remote Sens Environ 130:136–152. doi:10.1016/j.rse.2012.11.007

Lee SH, Song CK, Baik JJ, Park SU (2009) Estimation of anthropogenic heat emission in the Gyeong-In region of Korea. Theor Appl Climatol 96:291–303

LeMone MA, Tewari M, Chen F, Dudhia J (2013) Objectively determined fair-weather CBL depths in the ARW-WRF model and their comparison to CASES-97 observations. Mon Weather Rev 141(1):30–54

Li M, Song Y, Huang X, Li J, Mao Y, Zhu T, Cai X, Liu B (2014) Improving mesoscale modeling using satellite-derived land surface parameters in the Pear River Delta region, China. J Geophys Res Atmos 119:6325–6346

Lo JCF, Lau AKH, Chen F, Fung JCH, Leung KKM (2007) Urban modification in a mesoscale model and the effects on the local circulation in the Pearl River Delta region. J Appl Meteorol Climatol 46(4):457–476

Miao S, Chen F, LeMone MA, Tewari M, Li Q, Wang Y (2009) An observational and modeling study of characteristics of urban heat island and boundary layer structures in Beijing. J Appl Meteorol Climatol 48:484–501. doi:10.1175/2008JAMC1909.1

Miao S, Chen F, Li QC, Fan SY (2011) Impacts of urban processes and urbanization on summer precipitation: a case study of heavy rainfall in Beijing on 1 August 2006. J Appl Meteorol Climatol 50:806–825. doi:10.1175/2010jamc2513.1

Mlawer EJ, Taubman SJ, Brown PD, Iacono MJ, Clough SA (1997) Radiative transfer for inhomogeneous atmospheres: RRTM, a validated correlated-k model for the longwave. J Geophys Res Atmos 102:16663–16682. doi:10.1029/97jd00237

Narumi D, Kondo A, Shimoda Y (2009) Effects of anthropogenic heat release upon the urban climate in a Japanese megacity. Environ Res 109:421–431. doi:10.1016/j.envres.2009.02.013

Offerle B, Grimmond CSB, Fortuniak K (2005) Heat storage and anthropogenic heat flux in relation to the energy balance of a central European city centre. Int J Climatol 25:1405–1419. doi:10.1002/Joc.1198

Peng Z, Sun J (2014) Characteristics of the drag coefficient in the roughness sublayer over a complex urban surface boundary-layer. Meteorology. doi:10.1007/s10546-014-9949-8

Pigeon G, Legain D, Durand P, Masson V (2007) Anthropogenic heat release in an old European agglomeration (Toulouse, France). Int J Climatol 27:1969–1981. doi:10.1002/Joc.1530

Quah AKL, Roth M (2012) Diurnal and weekly variation of anthropogenic heat emissions in a tropical city, Singapore. Atmos Environ 46:92–103. doi:10.1016/j.atmosenv.2011.10.015

Sailor DJ (2011) A review of methods for estimating anthropogenic heat and moisture emissions in the urban environment. Int J Climatol 31:189–199. doi:10.1002/Joc.2106

Sailor DJ, Lu L (2004) A top–down methodology for developing diurnal and seasonal anthropogenic heating profiles for urban areas. Atmos Environ 38:2737–2748

Salamanca F, Martilli A, Tewari M, Chen F (2011) A study of the urban boundary layer using different urban parameterizations and high-resolution urban canopy parameters with WRF. J Appl Meteorol Climatol 50(5):1107–1128

Smith C, Lindley S, Levermore G (2009) Estimating spatial and temporal patterns of urban anthropogenic heat fluxes for UK cities: the case of Manchester. Theor Appl Climatol 98:19–35. doi:10.1007/s00704-008-0086-5

Sugawara H, Narita K (2009) Roughness length for heat over an urban canopy. Theor Appl Climatol 95:291–299. doi:10.1007/s00704-008-0007-7

Taha H (1997) Urban climates and heat islands: albedo, evapotranspiration, and anthropogenic heat. Energy Build 25:99–103. doi:10.1016/S0378-7788(96)00999-1

Trusilova K, Jung M, Churkina G, Karstens U, Heimann M, Claussen M (2008) Urbanization impacts on the climate in Europe: numerical experiments by the PSU-NCAR Mesoscale Model (MM5). J Appl Meteorol Climatol 47:1442–1455. doi:10.1175/2007jamc1624.1

Wang W (2009) The influence of thermally-induced mesoscale circulations on turbulence statistics over an idealized urban area under a zero background wind boundary-layer. Meteorology 131:403–423. doi:10.1007/s10546-009-9378-2

Wang Z, Wang X (2011) Estimation and sensitivity test of anthropogenic heat flux in Guangzhou. J Meteorol Sci (in Chinese) 31(4):422–430

Wang X, Liao J, Zhang J, Shen C, Chen W, Xia B, Wang T (2013) A numeric study of regional climate change induced by urban expansion in the Pearl River Delta, China. J Appl Meteorol Climatol 53:346–362

Yang L, Smith JA, Wright DB, Baeck ML, Villarini G, Tian F, Hu H (2013) Urbanization and climate change: an examination of nonstationarities in urban flooding. J Hydrometeorol 14:1791–1809. doi:10.1175/jhm-d-12-095.1

Zhang N, Gao ZQ, Wang XM, Chen Y (2010) Modeling the impact of urbanization on the local and regional climate in Yangtze River Delta, China. Theor Appl Climatol 102:331–342. doi:10.1007/s00704-010-0263-1

Zhang N, Chen Y, Zhao WJ (2012) Lidar and microwave radiometer observations of planetary boundary layer structure under light wind weather. J Appl Remote Sens 6.